ELSEVIER

Journal of Chromatography A, 740 (1996) 215–229

JOURNAL OF CHROMATOGRAPHY A

Absolute on-line molecular mass analysis of basic fibroblast growth factor and its multimers by reversed-phase liquid chromatography with multi-angle laser light scattering detection

Irina V. Astafieva[a,1], Gert A. Eberlein[b,2], Y. John Wang[b,*]

[a]*Wyatt Technology Corporation, 802 E. Cota St., Santa Barbara, CA 93103, USA*
[b]*Scios Nova Inc., 2450 Bayshore Parkway, Mountain View, CA 94043, USA*

Received 17 October 1995; revised 7 February 1996; accepted 8 February 1996

Abstract

The multi-angle laser light scattering (MALLS) detection method was combined with reversed-phase high-performance liquid chromatography to analyze multimerization of basic fibroblast growth factor (bFGF) formed by oxidation of bFGF with air or with 5,5′-dithio-bis(2-nitrobenzoic acid) (DTNB). This analysis provided the absolute molecular mass and the mean square radius for each eluted protein fraction or each slice of the chromatogram. It was shown that depending on the oxidation conditions, bFGF forms different multimeric forms, from dimers to hexamers. It was found that these multimers have varied conformations of the same molecular mass, but different structure. Molecular mass and size analyses provided molecular conformation of the aggregates; the results indicated the formation of rod-like rigid structures. The MALLS analysis confirmed that, during oxidation, each bFGF monomer bound sequentially to form the extended multimer. The proposed scheme of bFGF oxidation with DTNB revealed that the difference in the aggregate structural forms was probably due either to the presence of covalently bound residues of nitrobenzoic acid in the products of oxidation, or to the participation of sulfhydryl groups in disulfide bond formation.

Keywords: Molucular mass determination; Laser light-scattering detection; Detection, LC; Fibroblast growth factor; Dithio-bis(2-nitrobenzoic acid); Proteins

1. Introduction

Protein growth factors are known to induce the proliferation of a wide variety of mesoderm-derived cells, such as vascular endothelial cells. Basic fibroblast growth factor (bFGF) is one of many angiogenic factors which acts as a wound healing agent. Since bFGF was first isolated and identified from the hypothalamus, as an intracellular protein in its reduced form, it was believed that it also acts in a reduced form as a wound healing agent. However, there are new experimental data [1] which indicate that oxidized bFGF may be more active for cell proliferation in vitro than its reduced form. To prove the influence of oxidation on bFGF activity, it is necessary to characterize its different oxidation states. Since bFGF forms different types of aggregates on its pathway to the fully oxidized form,

*Corresponding author.
[1] Present address: Anergen, Inc., 301 Penobscot Dr., Redwood City, CA 94063, USA.
[2] Present address: Matrix Pharmaceuticals Inc., 1430 O'Brien Dr., Menlo Park, CA 94025, USA.

0021-9673/96/$15.00
PII S0021-9673(96)00134-3

aggregation becomes a major concern from the point of view of bFGF stability as a formulated drug. It was shown that identification of bFGF aggregates by size-exclusion chromatography (SEC) is difficult because of the non-ideal elution pattern of aggregated forms, as well as their interaction with the column support, which may alter their conformation [2]. We found that reversed-phase high-performance liquid chromatography (RP-HPLC) can efficiently separate different multimeric forms of bFGF.

The RP-HPLC method enables the separation of a wide range of proteins and pharmaceuticals, and it is capable of resolving different conformations, as well as monomers from their multimers. In contrast to SEC, the elution sequence in RP-HPLC does not correlate with molecular mass, or the size of the eluted molecules, but rather with their hydrophobicity. Since the way in which the conformation of protein multimers influences their hydrophobic interaction with a column matrix is generally unpredictable, no column calibration procedure can be used for the identification of unknown fractions on the basis of the retention volume or the mobile phase composition. Therefore, on-line identification and characterization of the separation, products is one of the most difficult problems in RP-HPLC. Frequently, one has to isolate each fraction and analyze it separately using an appropriate characterization method. However, the products of aggregation may participate in dynamic equilibria; in such a case, those components being separated and isolated might change their structure and molecular mass depending on the isolation procedure. Therefore, using a detector to measure the absolute molecular mass is especially important for reversed-phase chromatography applications, since it allows one to identify directly each eluted fraction.

Several techniques providing on-line molecular mass measurements for HPLC, including low-angle laser light scattering (LALLS) [3] and classic 90° light scattering (LS) detection [4] have been described before. Results published by Takagi and co-workers [5–8] and Krull and co-workers [3,9–15] show that LALLS, in combination with a UV and/or a refractive index detector (DRI), can be effectively used for molecular mass determination for a wide range of proteins and biopolymers. It was demonstrated that both LALLS and classic 90° LS detectors can be connected to SEC [3–9], RP-HPLC [10–14] or to ion-exchange HPLC [15]. These methods provide the molecular mass, however, they can not determine the size (i.e. radius) of eluted fractions. To be able to determine the size of the molecules, one needs to measure LS at different angles.

This paper describes multi-angle laser light scattering (MALLS) coupled with RP-HPLC, for absolute molecular mass measurements of bFGF and its multimers using the Wyatt miniDAWN detector. MALLS provides not only the absolute molecular mass, but also the size for each slice of the chromatogram, as well as the molecular mass and size distributions and their averages. This method provides the absolute molecular mass independently of the chromatographic conditions, elution volumes or the type of sample interaction with the column support. While MALLS has been applied to SEC of synthetic and biopolymers before, no work has been done on MALLS coupled with RP-HPLC.

2. Theory

Adding a MALLS instrument to a chromatography set-up allows the direct determination of absolute molecular mass and the size of the eluted molecules, on the basis of measurements of the excess Rayleigh ratio, R_θ, from an illuminated liquid sample at each scattering angle, θ, where

$$R_\theta = f[I(\theta) - I_s(\theta)]/I_0 \quad (1)$$

In Eq. (1) [16], f is a geometrical factor depending upon the field of view of the detector at the angle θ, the volume of the illuminated sample, and the geometry and refractive index of the scattering cell. At the angle θ, the intensity of scattered light detected from the illuminated sample is $I(\theta)$ and the scattered light intensity from the pure solvent is $I_s(\theta)$. The incident light intensity is I_0. In the limit of vanishingly small concentration, c, the excess Rayleigh ratio is related to the weight–average molecular mass $\bar{M}_w$ of the sample by [17,18]

$$\frac{R_\theta}{K^* c} = M_w P(\theta) + 2A_2 c \approx M_w P(\theta) \quad (2)$$

A_2 is the second virial coefficient, the function $P(\theta)$

is the scattering form factor which depends on the molecular configuration and the size, and whose value at $\theta=0$ is 1. Weight–average molecular mass $\bar{M}_w$ is a second statistical moment of molecular mass distribution:

$$\bar{M}_w = \sum(c_i M_i)/\sum c_i \quad (3)$$

where c_i and M_i are the concentration and molecular mass of the ith slice of the distribution, respectively. The sum is taken over one peak.

For vertically polarized incident light with a wavelength in vacuum λ_0, the optical constant K^* is given by

$$K^* = \frac{4\pi^2 n_0^2}{\lambda_0^4 N_A}\left(\frac{dn}{dc}\right)^2 \quad (4)$$

where dn/dc is the specific refractive index increment, n_0 is the refractive index of the solvent, and N_A is Avogadro's number.

For rather small molecules (10–30 nm), the scattering function can be approximated by [19]

$$P(\theta) = 1 - \frac{16\pi^2}{3\lambda^2}\langle r_g^2\rangle \sin^2(\theta/2) \quad (5)$$

where $<r_g{}^2>$ is the root mean square (rms) radius of the molecules. For larger molecules, more terms containing higher powers of $\sin^2(\theta/2)$ are required.

Combining Eq. (2) and Eq. (5), one can get the following relationship which is used for direct determination of molecular mass and size in MALLS experiments:

$$\frac{K^* c}{R_\theta} = \frac{1}{\bar{M}_w}\left[1 = \frac{16\pi^2}{3\lambda^2}\langle r_g^2\rangle \sin^2(\theta/2)\right] \quad (6)$$

For higher solute concentrations, correction factors (virial coefficients) must be applied [17]; this will introduce a concentration-dependent term into Eq. (6). Usually chromatography experiments are performed on solutions of low enough concentrations that the virial coefficients can be neglected.

On the basis of Eq. (6), molecular mass calculations are performed by extrapolation of the reciprocal scattering function $K^* c/R_\theta$, obtained for each point of the chromatogram, to zero scattering angle. The rms radius for each eluted fraction is determined from the slope of the angular dependence of this function.

It should be noted that the lowest rms radius which can be measured by MALLS is 8–15 nm. The reason for this limitation is that both the difference between scattering intensities at different angles (i.e. the slope) and the LS signal decrease with decreasing size of the molecules. At the same time, the level of noise remains constant. Therefore, for molecules below a certain size, the signal-to-noise ratio becomes too low to measure the slope. Reducing the noise by properly filtering the solvents and stabilizing the system made it possible for us to nearly reach the practical limit of lowest measurable rms radius of around 8 nm.

Classical LS theory is strictly valid for two-component systems [20]. However, in gradient elution, the mobile phase composition changes constantly. Therefore, at each elution point the system should be considered a multicomponent system under dynamic conditions. In this case, the optical constant K^* will change with elution volume depending on the change in solution refractive index. The validity of the LS method for three-component systems was intensively studied in the literature [21,22]. The most important conclusion with regards to the limits of validity of classical theory is that a three-component system can be artificially manipulated as a two-component system under certain assumptions and conditions. For systems under osmotic equilibrium, the refractive index increment corrections become insignificant for solvents having similar refractive indices, and those solvents can be regarded as isorefractive. It was shown that a three-component system containing an aqueous buffer (component 1), a protein (component 2) and an organic modifier (component 3) can be treated in LS measurements as a two-component system composed of a solvent and a protein, if the difference in refractive indices of two solvent components (n_1-n_3) fits the following relationship [22]:

$$(n_1 - n_3) < 0.025\,(dn/dc_2)(1/\gamma_3) \quad (7)$$

where dn/dc_2 is the specific refractive index increment of protein in aqueous buffer (i.e. dn/dc), and γ_3 is the specific interaction parameter of the organic modifier with the protein. This approach of isorefractivity was used by Krull and co-workers for protein

characterization using LALLS in combination with gradient elution. They demonstrated that for a system with a typical dn/dc_2 value of 0.15 ml/g and a small $\gamma_3 = 0.10$ ml/g, the solvents can be considered as isorefractive, if the absolute value of $(n_1 - n_3)$ is less than 0.038 [12].

3. Experimental

3.1. Instrumentation and experimental conditions

The chromatographic system consisted of a Hewlett-Packard 1050 HPLC System including a quaternary pump, degasser, auto injector and UV-DAD detector, as well as a miniDAWN instrument (Wyatt Technology, Santa Barbara, CA, USA). A Protein C_4 150×4.6 mm, 5 μm, 300 Å column (Vydac, Hesperia, CA, USA) with a flow-rate of 0.7 ml/min was used. An UV signal was recorded at 277 nm.

The miniDAWN measures the LS at 45°, 90° and 135° (these values vary with the solvent refractive index). The flow-through refraction cell allows these angular measurements to be made on a relatively small scattering volume (1 μl), without excess scattering from the glass–solvent interfaces where the laser enters and leaves the cell. The 20 mW solid-state diode laser emits a vertically polarized beam at a wavelength of 690 nm which is collimated in the center of the cell.

The miniDAWN instrument was placed after the UV detector. The miniDAWN calibration constant was measured with toluene before the instrument was attached to the chromatography system. The responses of the photodiodes were normalized using an injection of a small-size protein sample that scattered light isotropically, namely the bFGF monomer. The delay volume between the LS instrument and the UV detector was measured and found to be 0.04 ml using a procedure described earlier [23]. Data were recorded and processed using Wyatt Technology's ASTRA chromatography software version 1.2 for the Macintosh. The UV detector calibration constant was obtained using a bFGF monomer sample with a known concentration. It was assumed that all the multimers had the same absorptivity as the monomer.

Two mobile phases were used for gradient elution. The first mobile phase consisted of 0.1% trifluoroacetic acid (TFA) in HPLC-grade water (A); the second mobile phase consisted of 0.09% TFA in acetonitrile–water (50:50, v/v) (B). All mobile phases were filtered with a 0.1-μm Anodisc membrane filter (Alltech, Deerfield, IL, USA) using a standard laboratory vacuum filtration procedure. The gradients used for RP-HPLC experiments are presented in the Table 1. The protein Vydac C_4 column was first flushed with mobile phase B for 2 h, and further equilibrated with mobile phase A for 24 h.

3.2. Sample preparation

Recombinant bFGF (FM = 17 124) was produced at Scios Nova by the recombinant bacterial expression method in *E. coli* as described by Thompson et al. [24]. The following solutions were used for sample preparation:

The bFGF stock solution contained 3.63 mg/ml ($211 \cdot 10^{-6}$ mol/l) bFGF in 20 m*M* citrate buffer, pH 5.0, 9% sucrose and 2 m*M* Na_2EDTA; it was stored at −80°C. Placebo buffer was prepared by adding 20 ml of a 200 m*M* Na_2HPO_4 base (pH 8.4) to 20 ml of

Table 1
Gradient conditions used for RP-HPLC

Gradient 1			Gradient 2			Gradient 3		
Time (min)	B (%)	A (%)	Time (min)	B (%)	A (%)	Time (min)	B (%)	A (%)
0	0	100	0	0	100	0	0	100
5	56	44	5	46	54	3	20	80
25	76	24	15	56	44	15	46	54
35	80	20	35	76	24	45	76	24
40	0	100	45	76	24	50	80	20
			50	0	100	55	0	100

Where A is 0.1% TFA in HPLC-grade water, B is 0.09% TFA in acetonitrile–water (50:50, v/v).

a buffer solution containing 10 m*M* sodium citrate, 2 m*M* Na_2EDTA, 9% sucrose, pH 5.0, to give a final concentration of 100 m*M* Na_2HPO_4, 5 m*M* citrate buffer, 1 m*M* Na_2HPO_4, 4.5% sucrose, pH 7.8. The final solution of bFGF (used for oxidation by aeration) was prepared by adding 2.5 ml of 200 m*M* Na_2HPO_4 base (pH 8.4) to 2.5 ml of bFGF stock solution. The final concentrations were 1.82 mg/ml ($233 \cdot 10^{-9}$ mol/l) bFGF, 100 m*M* Na_2HPO_4, 5 m*M* citrate buffer, 1 m*M* Na_2EDTA and 4.5% sucrose.

DTNB [5,5′-dithio-bis(2-nitrobenzoic acid)] solution (10-fold excess over bFGF) was made by dissolving 2.592 mg DTNB in 10 ml placebo buffer, in order to obtain a final concentration of 0.288 mg/ml DTNB ($727 \cdot 10^{-9}$ mol/l), 100 m*M* Na_2HPO_4, 5 m*M* citrate buffer, 1 m*M* Na_2HPO_4, 4.5% sucrose, pH 7.8.

Multimeric forms of bFGF were prepared using two oxidation methods; (1) with oxygen from air, i.e. aeration and (2) with DTNB. For air oxidation, the bFGF solution was stored for three months at 4°C. Oxidation products were separated and purified by heparin affinity chromatography using Toso Haas Heparin-5PW column (75×7.5 mm, 10 $\mu M \times 1000$ Å, Type HE5PH0124) at a flow-rate of 1.0 ml/min and by loading 50 μl (30 μg) of the sample. The first mobile phase was 100 m*M* potassium phosphate, 1 m*M* Na_2EDTA, pH 6.5 and the second mobile phase contained 3 *M* NaCl in the first mobile phase. The elution gradient was 180 m*M* NaCl/min. We collected fractions corresponding to single peaks. These fractions were further analysed with RP-HPLC.

To perform bFGF oxidation by DTNB, we mixed the final bFGF solution with the DTNB solution at a particular molar ratio φ, adding the placebo buffer to obtain a final concentration of bFGF of 1.01 mg/ml (0.06 m*M*) in 100 m*M* Na_2HPO_4, 10 m*M* citrate buffer, 1 m*M* EDTA, 4.5% sucrose, pH 7.8. The degree of bFGF oxidation corresponds to the number φ of DTNB equivalents added:

$$\varphi = [\text{DTNB}]/[\text{bFGF}]$$

where [DTNB] and [bFGF] are molar concentrations of DTNB and bFGF. The products of bFGF oxidation with DTNB were analysed using RP-HPLC without any further purification.

We injected 70–100 μl of bFGF samples that were oxidized by air and 100–120 μl of the samples oxidized with DTNB. Each sample was injected at least twice under the same conditions, without filtration.

4. Results and discussion

The purpose of this study was to determine the absolute molecular mass of bFGF and its multimers formed by oxidation of the native protein, using the MALLS detection method connected to RP-HPLC. This study includes the development of the MALLS method for gradient elution conditions, analysis of bFGF oxidized at different oxidation conditions, characterization of different conformations of bFGF multimers, determination of their molecular mass and size values, and discussion of the proposed scheme of bFGF oxidation with DTNB.

4.1. Effect of solvent gradient on the light scattering signal

Reversed-phase chromatography applies gradient elution and, therefore, uses mixed solvents. The intensity of the LS signal is determined by the Rayleigh ratio of the solvent and solutes (which reflects their ability to scatter light) and on the solute concentration. Since the LS signal depends on the refractive index of the solvent, the change in solvent composition will directly influence the LS intensities. This is illustrated in Fig. 1. One can see that the increasing concentration of acetonitrile in water causes an increasing LS baseline. Moreover, the LS baseline corresponds exactly to the solvent gradient. This behavior is due to the difference in the ability of acetonitrile and water to scatter light; acetonitrile has a much higher Raleigh ratio than water. A linear change in the mobile phase composition gives a linear change in the LS signal. One can note that the LS chromatograms obtained using RP-HPLC are very different from those obtained with SEC. Since SEC uses an isocratic elution, the baselines of LS chromatograms at different scattering angles look similar to those of refractive index or UV signals, i.e.

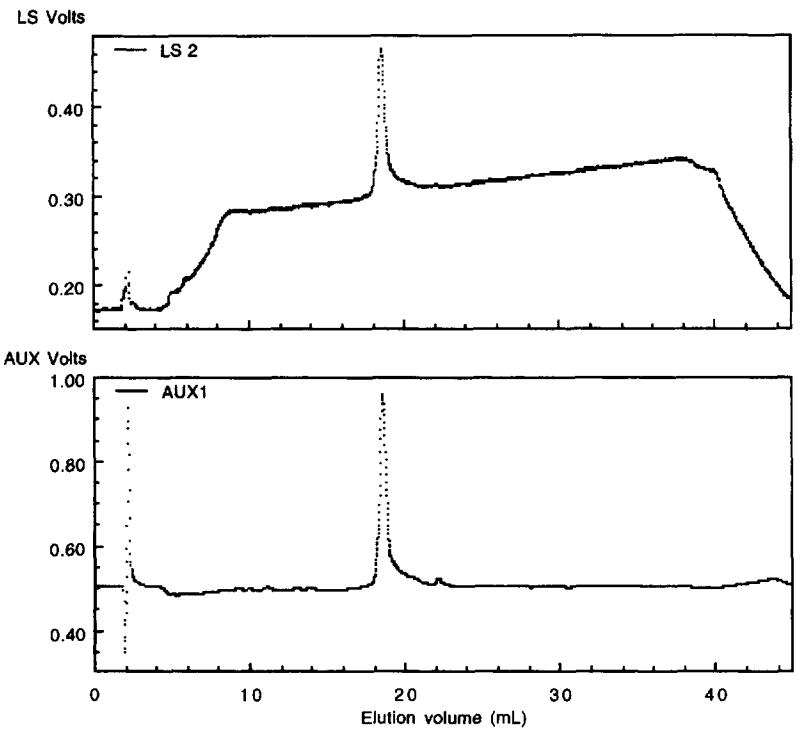

Fig. 1. Light scattering at 90° (LS2) and UV at 277 nm (AUX1) signals for bFGF trimer obtained by oxidation with air.

flat. In contrast, with a gradient elution, the baselines of LS signal reflect the solvent gradient profile being used and the LS chromatograms may look different from UV chromatograms. To process these data, the LS baselines were set at the linear region of the chromatograms (starting before the peaks and ending after the peak). Fig. 2 shows the chromatograms of a LS signal at 90° overlaid with an UV signal at 277 nm, after subtraction of the baselines.

Different gradient conditions were used to optimize RP-HPLC experiments. The critical gradient interval was kept without change at 56–76% mobile phase B over 20 min. Other conditions, such as slope and duration of the gradient before and after this interval, varied. It was found that the initial increase of acetonitrile concentration before the critical interval does not influence the shape and resolution of the LS and UV peaks of the bFGF multimer mixtures. Thus, using gradients 2 and 3 (Table 1) gave the same results for eluted bFGF fractions as those obtained using gradient 1. When the longer linear gradient of the same rate was used, the LS signal had a longer linear range, which helped to verify the linearity of the LS response with changing solvent composition. We found that the Vydac C_4 column could be flushed rather quickly with the first mobile phase after the applied gradient; the drop of the mobile phase B composition from 80 to 0% did not cause any distortion in the LS signal at any angle. The LS chromatograms for several consecutive runs were highly reproducible.

We showed that premixing of the first mobile phase with a small amount of acetonitrile (2%) resulted in smoother baselines for gradient elution, when the column was hooked up initially. We found that several fast gradient runs "condition" the column and flushed out all previously adsorbed species. After this procedure, one can use either version of the first mobile phase and get the same results. All the experiments described here were performed using gradient 1, since it took less time for each run and provided good performance.

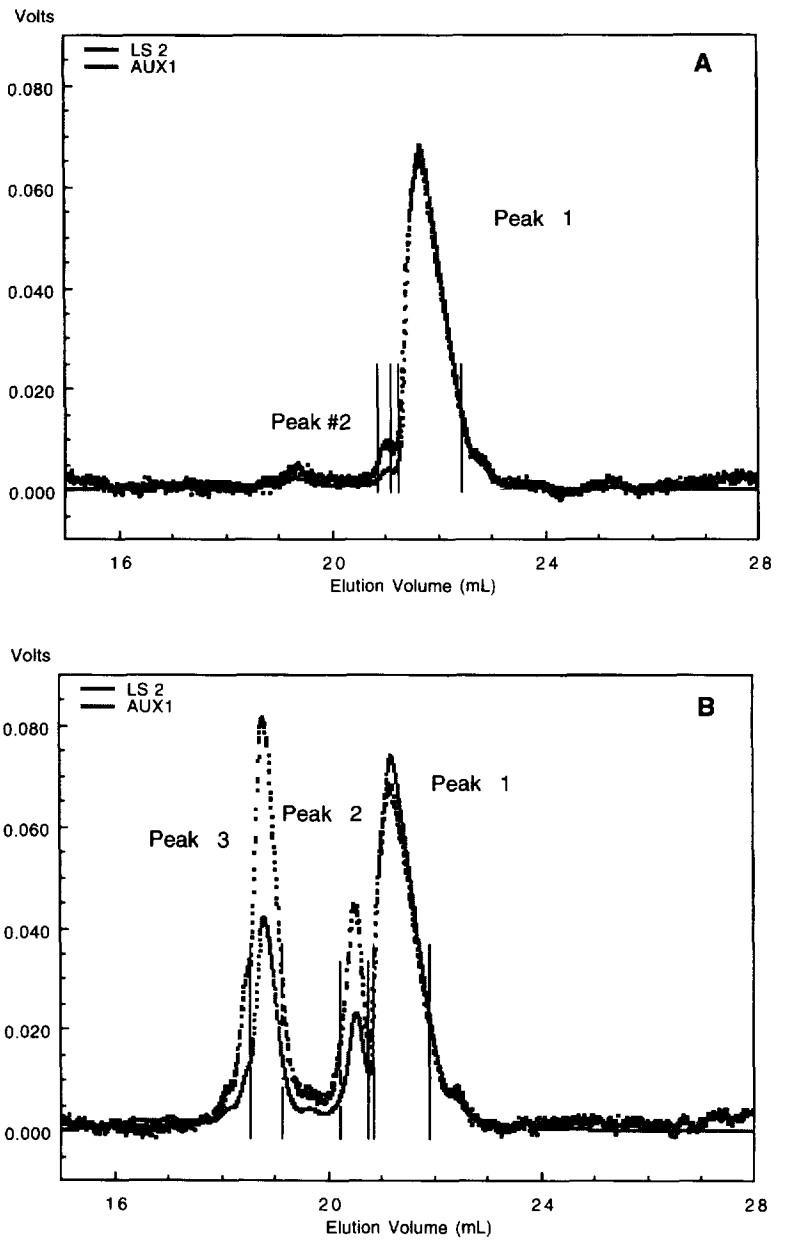

Fig. 2. Light scattering at 90° (LS2) and UV at 277 nm (AUX1) signals overlaid after subtraction of the baselines for bFGF monomer (A) and for the product of bFGF oxidation with DTNB, $\varphi = 0.2$ (B). The UV (AUX1) tracings are the lower curve in panel A; and the upper curve of peak 1 and the lower curve of peaks 2 and 3 in panel B.

4.2. Determination of the dn/dc value for bFGF

To determine the molecular mass for each eluted protein fraction, one needs to know the dn/dc value (refractive index increment of solute in solution) and the concentration for each slice of the peak.

The dn/dc value depends on the chemical nature of the dissolved species, as well as on the solvent. As

discussed in section 2, a three-component system can be manipulated as a two-component system, if the difference in refractive indices of two solvent components (n_1-n_3) fits the value determined from Eq. (6). The refractive index of water at pH 3 is 1.332, and the value of acetonitrile at the same pH is 1.341 (at 25°C and 633 nm). The difference in refractive indices of mobile phases A and B is 0.009, which is well below the value that allows solvents to be considered as isorefractive. Moreover, the elution of different protein fractions occurred in the linear gradient region where the concentration of acetonitrile changed from 34 to 38%, which caused the refractive index to change by less than 0.0004.

Two different approaches were used to determine the dn/dc values. Both approaches assume that each eluted protein fraction has the same dn/dc and absorptivity values. Since all the fractions were eluted in the narrow interval of the mobile phase compositions, this assumption could not introduce more than a 3–4% error in the dn/dc values. The first approach was based on the assumption that the dn/dc value of bFGF is close to the value of other proteins. As was previously shown by Mhatre et al. [12,15], individual dn/dc values for RNase A, lysozyme and BSA, at various mobile phase compositions containing aqueous buffer and acetonitrile, were very similar. Based on these data, we used a dn/dc value of bFGF and its multimers of 0.175 ml/g. Using this value, protein recovery was determined to be around 90–96% from the column, for all bFGF samples. The second approach to determine the bFGF dn/dc value assumed that all the injected monomer bFGF sample was completely recovered from the column. This approach also assumed that the sample did not have any contaminants and that the protein concentrations were measured precisely. Using both approaches we got similar results for the bFGF dn/dc value of 0.175 ± 0.004 ml/g and this value was used in all calculations. Since the LS signal is proportional to the $(dn/dc)^2$ value, both assumptions may give an error of not more than 4–5% in the molecular mass values.

4.3. Molecular mass and size determination with MALLS

Fig. 2 shows the chromatograms of LS at 90° and UV at 277 nm overlaid (after the baseline subtraction) for two bFGF samples. The first plot (Fig. 2A), showing the chromatograms for the native purified protein (bFGF monomer), indicates that the main peak elutes at 22 ml and a small pre-peak at 21 ml. It also shows that the ratios of intensities of the LS and the UV signals on the top of the two peaks are different. The second plot (Fig. 2B), shows the chromatograms for bFGF oxidized with 0.2 equivalents of DTNB. It shows three peaks of different intensities. The last peak appears at an elution volume that is close to that of the bFGF monomer, and has a similar shape. One can see that the LS signal for the first two peaks is approximately twice the UV signal, while for the third peak the two signals are equal.

As was shown in Section 2, the LS signal is proportional to the product of the molecular mass and concentration, while the UV signal is proportional to concentration alone. Therefore, one can estimate the molecular mass simply from the ratio of the LS and UV signals. Chromatograms presented in Fig. 2B clearly indicate that the two first eluted fractions (peaks 3 and 2) have similar molecular masses, which are higher than the molecular mass of the last fraction (peak 1). The molecular mass analysis shows that the three peaks in Fig. 2B correspond, from left to right, to two types of dimers and to a single monomer of bFGF. The fact that the LS signal is proportional to molecular mass results in higher intensities of the LS signal for the multimers and also explains the sensitivity of the LS method to the presence of aggregates.

The molecular mass values for eluted fractions were calculated for the portions of the peaks which lie within the peak ranges, as shown in Fig. 2. These ranges were defined by the common detection limit for the MALLS and UV chromatograms in the peak regions. The plots of molecular mass vs. elution volume obtained directly from these sample runs are shown in Fig. 3A. The weight–average molecular mass defined in Eq. (3) for the bFGF monomer sample is 17 000 g/mol and the three peaks of bFGF oxidized with 0.2 equivalents of DTNB have 35 000 g/mol for the first peak, 34 000 g/mol for the second and 17 000 g/mol for the third peak.

Fig. 3B shows the cumulative molecular mass distribution plots of these two bFGF samples. The cumulative molecular mass distribution shows the dependence of the weight fraction vs. the molecular

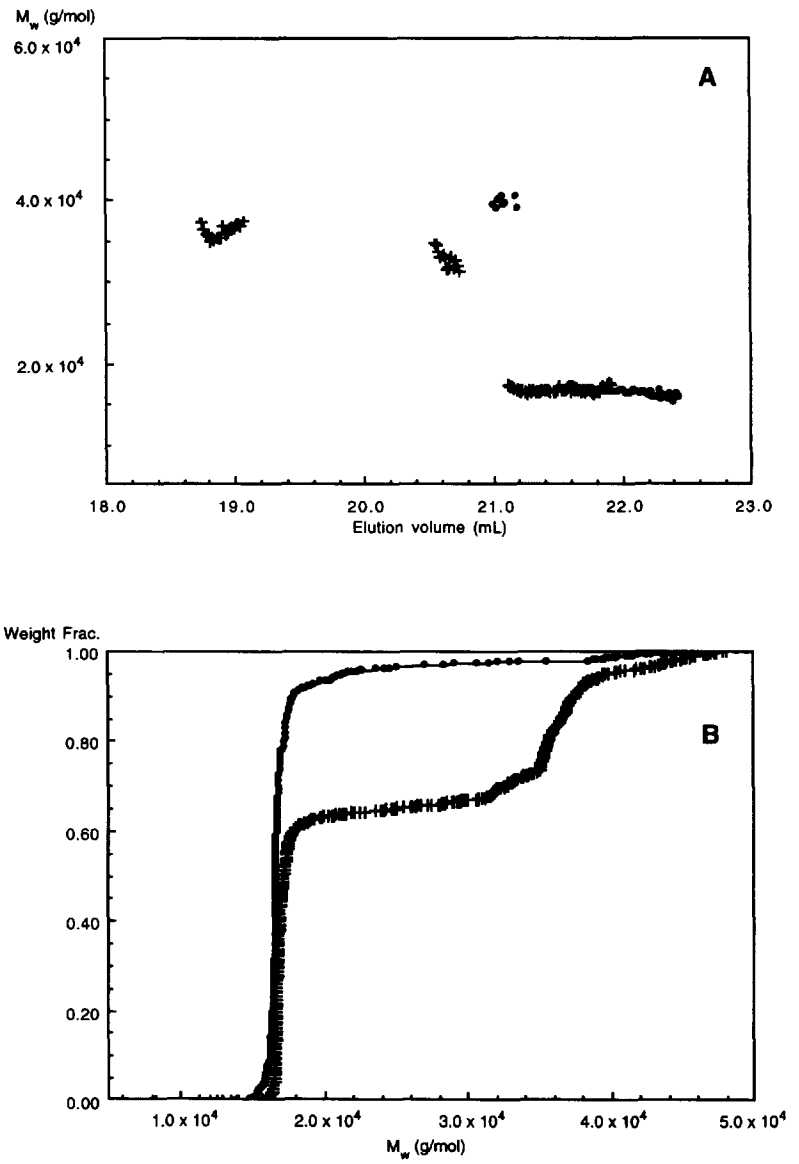

Fig. 3. (A) Plot of molecular mass vs. elution volume and (B) cumulative molecular mass distribution plot for bFGF monomer (closed circles) and bFGF oxidized with 0.2 equivalents of DTNB (crosses).

mass. Each step of this distribution plot indicates a fraction of a sample (i.e. a component of the mixture); the position of the vertical part of the step shows the molecular mass of a fraction, and the height of the step shows the amount of the material in this fraction. One can see that the bFGF monomer sample shows the main step on this plot, with a very steep slope and a height of around 95%. This indicates that this sample is mostly monodisperse and contains about 95% of the monomer. In contrast to the bFGF monomer, the sample oxidized with 0.2 equivalents of DTNB protein has at least two main steps. This indicates the presence of two main fractions having different molecular masses. Thus, the first fraction contains the monomer at around 65% and the second step is the dimer. One can note that the cumulative plot does not distinguish the different conformations of the aggregates having the

same molecular mass. The combination of the molecular mass vs. elution volume plot and the cumulative molecular mass distribution plot provide a complete quantitative characterization of the samples.

Fig. 4 shows an example of molecular mass and rms radius calculations for one of the bFGF oxidation products. LS data obtained for three LS angles are plotted vs. $\sin^2(\theta/2)$ in Fig. 4A, for a chosen slice of the chromatogram shown in Fig. 4B. Molecular mass calculations were performed by extrapolation of the reciprocal scattering function K^*c/R_θ obtained for each point of the chromatogram, to zero scattering angle. Root mean square radius for each eluted fraction was determined from the slope of the angular dependence of this function. One can see that for the chosen slice at the elution volume of 18.75 ml, corresponding to the maximum of the first peak, the molecular mass value is 84 700±500 g/mol and the rms radius is 13±2 nm. The standard deviation values shown with the results are calculated, by the software for each data point of the chromatogram, on the basis of the detector noise (shown in the plot of K^*c/R_θ vs. $\sin^2(\theta/2)$ with the error bars), and its effect on the linear fit.

The data shown in Fig. 4 were obtained for bFGF oxidized with air and purified by heparin affinity chromatography. The calculated molecular mass value for the chosen chromatographic peak indicates a pentamer. If one assumed a globular conformation for this multimer, the radius for the pentamer would be around 4 nm. This value is supported by the crystallographic determination of the triclinical crystal of bFGF, with the cell dimensions of 3.3, 3.5 and 3.1 nm [25]. However, for the bFGF pentamer in solution, a rms radius obtained with MALLS mea-

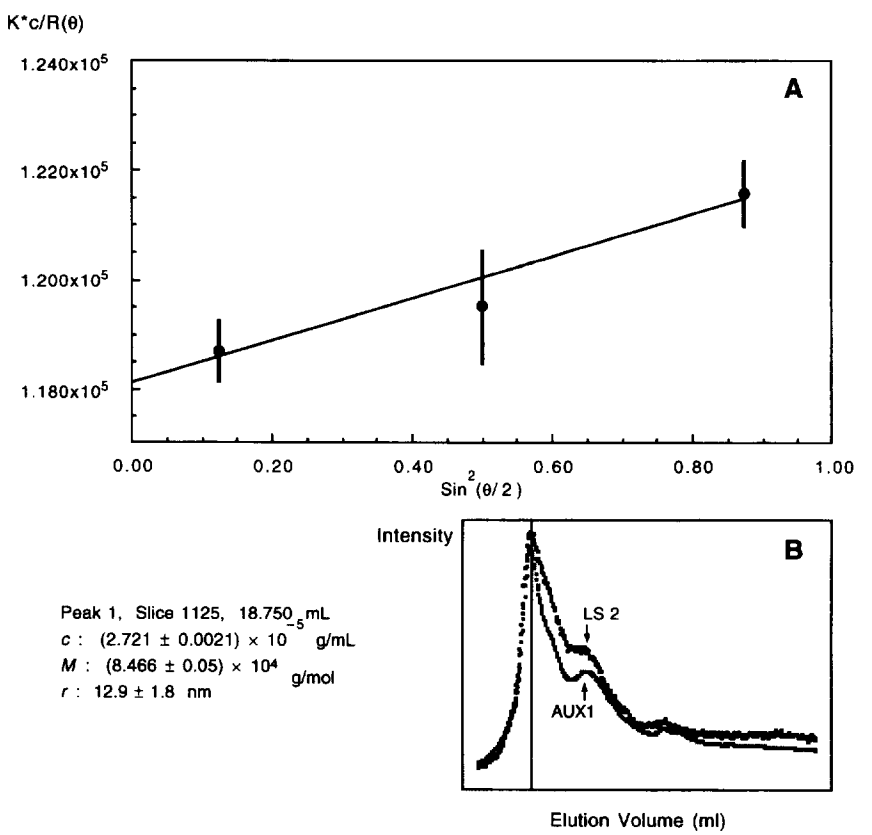

Fig. 4. Example of the calculation of molecular mass and rms radius for bFGF pentamer; a Debye plot showing the angular dependence of the reciprocal scattering function (A) for a chosen slice of a chromatogram showing both light scattering and UV signals overlaid (B).

surements from the angular dependence of the LS signal is much higher, i.e., 13 nm. The molecules with a molecular mass of about 85 000 g/mol may have a radius of 13 nm only if they have a rather extended conformation, i.e., as a stiff chain or a rod. One can see that the MALLS method, in contrast to LALLS, provides an independent measurement of two characteristic molecular parameters; the molecular mass and the size. The MALLS method, therefore, can give information concerning the conformation of the samples. Thus, the results obtained for bGFG multimers indicate their rod-like conformation. On the basis of these data, we propose a probable mechanism of bFGF oxidation which suggests that each monomer binds sequentially to form the extended rigid multimer. This mechanism will be discussed in detail later.

4.4. Characterization of the bFGF oxidation products. Different multimer conformations

The chromatograms shown in Fig. 2B for bFGF oxidized with 0.2% of DTNB show two different dimers eluting at different elution volumes. The fact that the two fractions having the same molecular weight elute at different solvent compositions indicates that they have different hydrophobicities and, therefore, different structures.

Fig. 5 presents LS and UV chromatograms overlaid for bFGF samples oxidized with greater amounts of DTNB, i.e., 1.1 and 4 equivalents. These chromatograms show multiple peaks for both samples. The molecular masses and the amounts of all fractions for the bFGF samples oxidized with DTNB are summarized in Table 2. The results of the molecular mass analysis show that bFGF oxidized with the equivalent amount of DTNB contains two different dimers and two trimers, as well as a monomer. At an excess of DTNB (4 equivalents) bFGF forms a monomer which elutes at a much higher concentration of the second mobile phase than the native form. This indicates that over-oxidized bFGF forms a monomer which is more hydrophobic than the native bFGF monomer. We assume that this difference in structure is probably due to the presence of covalently bound nitrobenzoic acid or to the internal disulfide bond formation. This will be discussed in detail in section 4.5.

The molecular mass vs. elution volume plot presented in Fig. 6 shows the results of the MALLS analysis for bFGF samples oxidized with air, as well as of non-oxidized bFGF monomer. These samples of oxidized bFGF have been separated and purified with heparin affinity chromatography prior to RP-HPLC. Each of them contained the molecules of the same molecular mass after purification. However, one can see that each of these samples shows more than one band of the same molecular mass at the different elution volumes. Thus, the sample of bFGF trimer contains three different trimers. The same is true for tetramers, pentamers and hexamers. One can see that there is no correlation between the elution volume and the molecular mass; for example, the pentamers elute at both lower and higher elution volumes than the monomer and, therefore, have different hydrophobicities. These data show that the oxidized bFGF multimers form different conformations.

4.5. Scheme of bFGF oxidation with DTNB

To explain the formation of different conformations of bFGF multimers, we propose a scheme of bFGF oxidation with DTNB. This scheme is presented in Fig. 7. Since the scheme shows the oxidation mechanism with DTNB as an oxidation agent, it considers only oxidation of the sulfhydryl groups of the protein.

bFGF has four sulfhydryl groups. Two of them are accessible for oxidation by disulfide bond formation, but they are located too far apart to interact with each other and form intramolecular disulfide bonds. The two other disulfide groups are buried in the structure and can form disulfide bonds only after denaturation.

DTNB is a selective two-electron transfer agent; it has a very low transition energy in most sulfide–disulfide electron transfer reactions and it provides fast and complete reactions. Its redox potential favors the oxidation of most SH-bonds, especially in proteins, leading to intramolecular or intermolecular disulfide bonds, as well as to the formation of mixed adducts containing a nitrothiobenzoic acid group attached to one of the oxidized sulfhydryl groups. A low activation energy of these reactions makes oxidation with DTNB preferable in comparison with

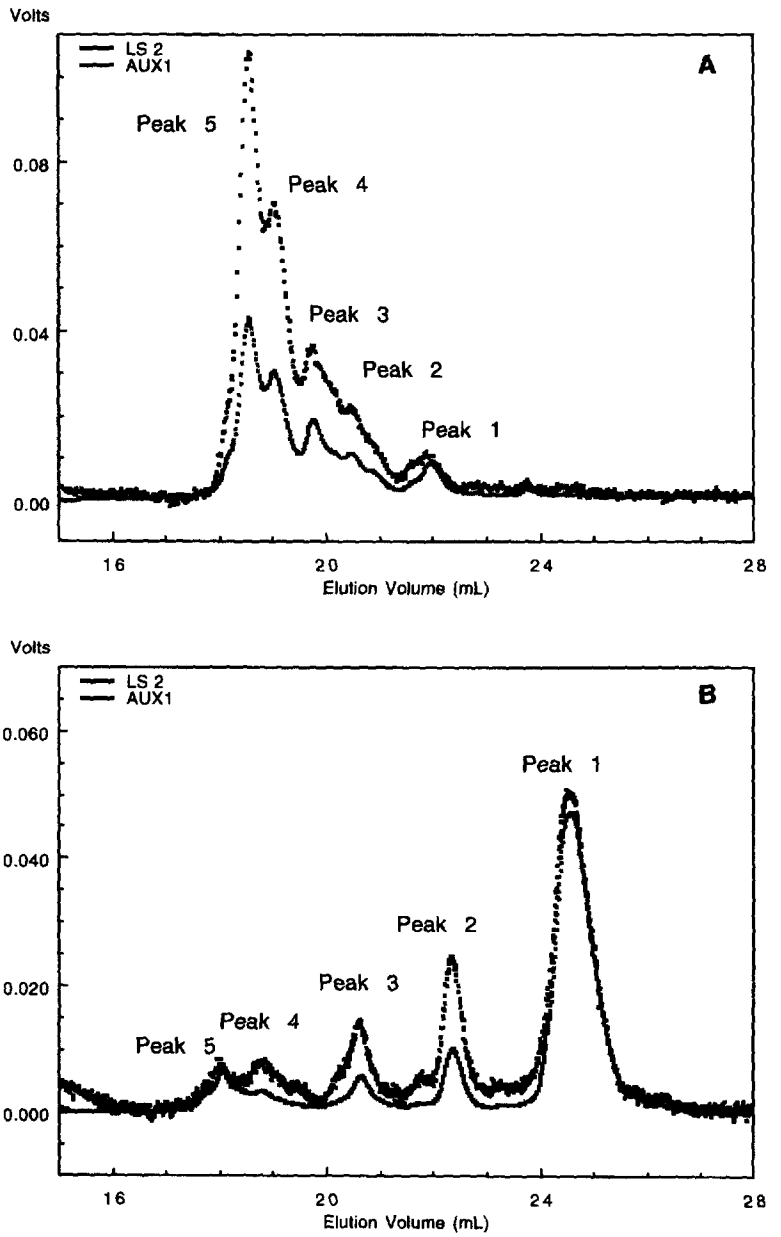

Fig. 5. Light scattering at 90° (LS2) and UV at 277 nm (AUX1) signals overlaid after subtraction of the baselines for the products of bFGF oxidation with DTNB: $\varphi = 1.1$ (A) and $\varphi = 4$ (B). The lower curves are from the UV signal (AUX1).

the slow, air–oxygen oxidation. Moreover, DTNB specifically oxidizes only SH-groups, it does not oxidize tryptophan, tyrosine, methionine or other amino acids. In contrast to this, the oxidation with air–oxygen is not specific (it is a radical chain reaction). Oxygen may oxidize not only SH-groups, but also methionine, and probably, tryptophan, forming many oxidation products.

The scheme in Fig. 7 shows that DTNB oxidizes the two sulfhydryl groups of bFGF either to the dimer, or to its adduct with thionitrobenzoic acid. Increasing the amount of DTNB increases bFGF

Table 2
Characteristics of the bFGF oxidation products separated and analyzed with RP-HPLC coupled with MALLS and UV detectors

Equivalents of DTNB added, φ	Peak number (in Fig. 2 and Fig. 5)	Elution volume at the top of the peak (ml)	M_w of the peak (g/mol)	Fraction amount (%)
0	1	21.68	$(1.71\pm0.02)10^4$	94
	2	21.04	$(3.8\ \pm0.1\ )10^4$	3
	3	19.32	$(3.0\ \pm0.3\ )10^4$	3
0.2	1	21.24	$(1.70\pm0.03)10^4$	63
	2	20.56	$(3.41\pm0.08)10^4$	11
	3	18.80	$(3.5\ \pm0.1\ )10^4$	26
1.1	1	21.97	$(1.70\pm0.03)10^4$	10
	2	20.47	$(3.52\pm0.08)10^4$	12
	3	19.77	$(3.8\ \pm0.2\ )10^4$	19
	4	19.06	$(5.1\ \pm0.1\ )10^4$	24
	5	18.16	$(5.3\ \pm0.1\ )10^4$	35
4	1	24.56	$(1.78\pm0.04\ )10^4$	74
	2	33.36	$(3.4\ \pm0.1\ )10^4$	10
	3	20.62	$(3.5\ \pm0.2\ )10^4$	7
	4	18.81	$(3.3\ \pm0.3\ )10^4$	5
	5	18.05	$(1.8\ \pm0.1\ )10^4$	4

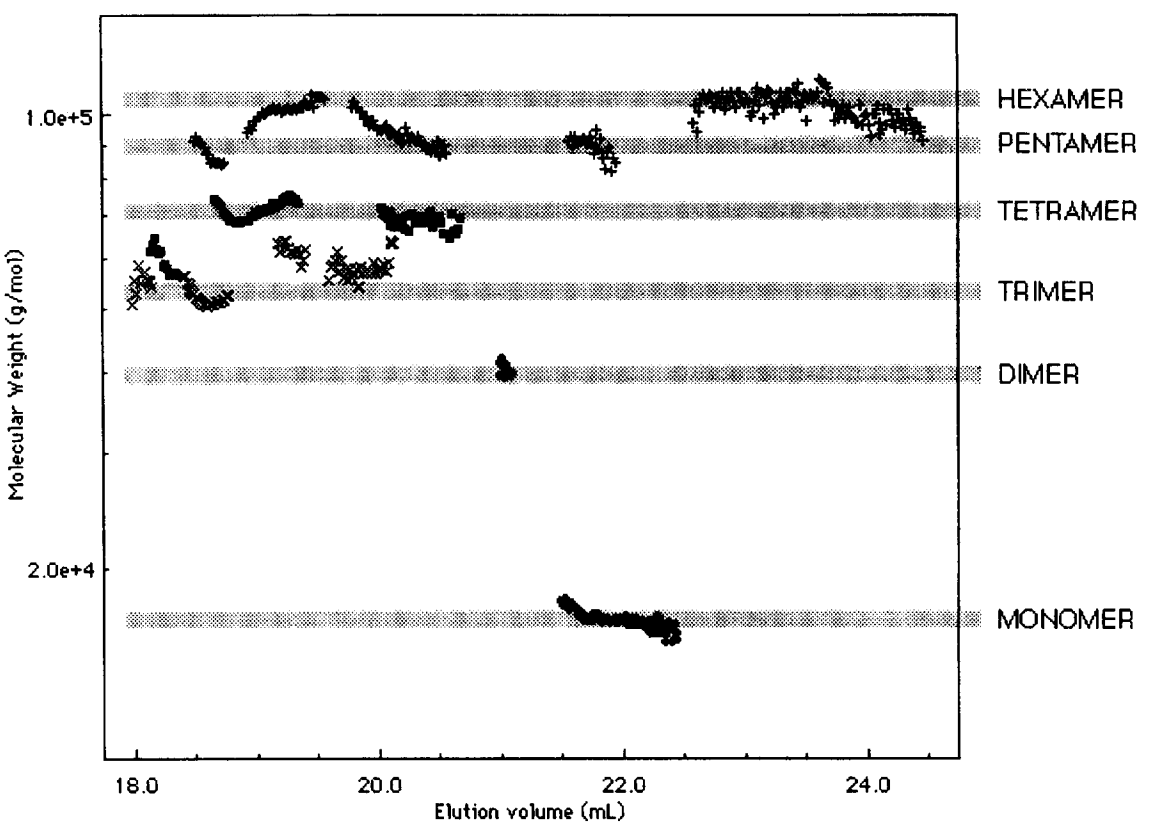

Fig. 6. Plot of molecular mass vs. elution volume for bFGF multimers obtained by oxidation with air.

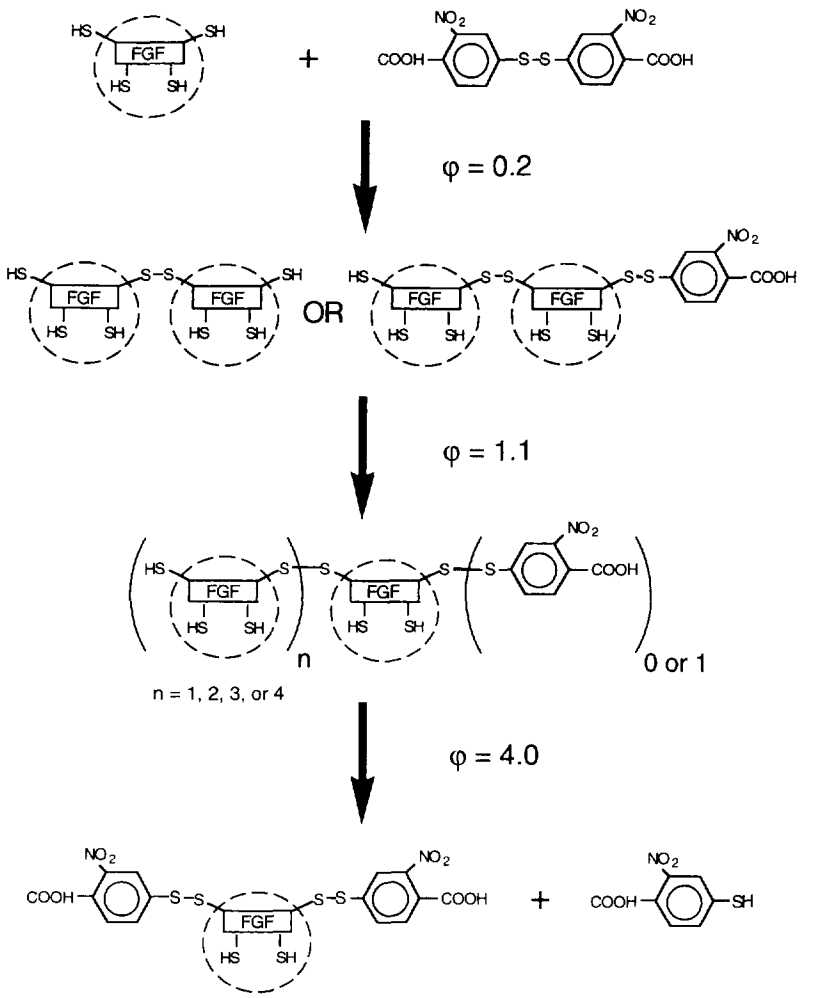

Fig. 7. Scheme of bFGF oxidation with DTNB.

multimerization and this process may lead to the formation of different structures, as well as to aggregates of different molecular mass. An excess of DTNB unfolds the protein and makes it possible to oxidize the previously buried sulfhydryl groups. This leads to the formation of a monomer with a different structure than that of the native form, i.e., a monomer modified with one or two thionitrobenzoic acid groups. The formation of the modified monomer was confirmed by studying the oxidation of denatured dimer.

The MALLS analysis revealed that the bFGF multimers must have a rod-like conformation. These data are in good agreement with the chemical structure of bFGF multimers shown in the scheme. The MALLS data confirm that each bFGF monomer binds sequentially to form the multimer. Depending on the amount of added DTNB and the oxidation conditions, the degree of conversion in the oxidation reaction can be different. Thus, the multimers of different molecular masses can coexist in the reaction mixture.

5. Conclusions

RP-HPLC in combination with MALLS was used to analyze the oxidation products of bFGF. The

native protein was oxidized by two different methods, i.e., non-specific oxidation by air and specific oxidation of sulfhydryl groups with DTNB.

It was shown that the MALLS method is compatible with reversed-phase gradient elution. MALLS combined with UV detection provides the absolute molecular mass and the radius for each eluted protein fraction, or for each data point of the chromatogram.

MALLS analysis detects the presence of different multimeric forms of oxidized bFGF depending on the oxidation conditions; from dimers to hexamers, as well as their varied conformations. Two different forms of dimer were detected at a low equivalent ratio of added DTNB ($\varphi = 0.2$). At a higher ratio ($\varphi = 1.1$), two different trimers and dimers were found. At an excess of DTNB ($\varphi = 4$), bFGF forms a monomer of different hydrophobicity than that of the native form. On the basis of the results obtained, we proposed a scheme of bFGF oxidation with DTNB, which explains the formation of different conformations of bFGF multimers. The difference in their structure is probably due to the presence of covalently bound residues of nitrobenzoic acid in the product of oxidation, or due to the participation of sulfhydryl groups in the formation of disulfide bonds.

The molecular size analysis performed with MALLS shows that the multimers must have a rod-like conformation. For example, a pentamer with a molecular mass of 85 000 g/mol has a relatively large rms radius of 13 nm. This would be possible only if the conformation is extended as a stiff chain or a rod. Thus, each monomer binds sequentially to form the extended rigid multimer.

Acknowledgments

The authors would like to thank Dr. Philip Wyatt and Lena Nilsson for their valuable comments and helpful discussions.

References

[1] R. Mischak, unpublished data.
[2] G. Eberlein, unpublished data.
[3] H.H. Stuting, I.S. Krull, R.M. Mhatre, S.C. Krzysko and H. Barth, LC·GC Mag., 7 (1989) 402.
[4] G. Dollinger, B. Cunico, M. Kunitani, D. Johnson and R. Jones, J. Chromatogr., 592 (1992) 215.
[5] T. Takagi, J. Chromatogr., 506 (1990) 409.
[6] A. Kato, K. Kameyama and T. Takagi, Biochim. Biophys. Acta, 1159 (1992) 22.
[7] Y. Sato, N. Ishikawa and T. Takagi, J. Chromatogr., 507 (1990) 25.
[8] Y. Kijima, T. Takagi, M. Shigekawa and M. Tada, Biochim. Biophys. Acta, 1041 (1990) 1.
[9] H. Stuting and I.S. Krull, Anal. Chem., 62 (1990) 2107–2114.
[10] D.J. Magiera and I.S. Krull, J. Chromatogr., 606 (1992) 264.
[11] I.S. Krull, H.H.Stuting and S.C. Krzysko, J. Chromatogr., 442 (1988) 29.
[12] R. Mhatre, I.S. Krull and H.H. Stuting, J. Chromatogr., 502 (1990) 21.
[13] H.H. Stuting and I.S. Krull, J. Chromatogr., 539 (1991) 91.
[14] R.M. Mhatre and I.S. Krull, J. Chromatogr., 591 (1992) 139.
[15] R.M. Mhatre and I.S. Krull, Anal. Chem., 65 (1993) 283.
[16] P.J. Wyatt and L.A. Papazian, LC·GC Mag., 11 (1993) 862.
[17] B.H. Zimm, J. Chem. Phys. 16 (1948) 1093.
[18] P.J. Wyatt, Anal. Chim. Acta, 272 (1993) 1.
[19] P.J. Wyatt, J. Chromatogr., 648 (1993) 27.
[20] M.B. Huglin, Light Scattering from Polymer Solutions, Academic Press, New York, 1972.
[21] P. Kratochvil, Classical Light Scattering from Polymer Solutions, Elsevier, Amsterdam, 1987, Ch. 4.
[22] H. Eisenberg, Biological Macromolecules and Polyelectrolytes in Solution, Clarendon Press, Oxford, 1976, p. 77.
[23] C. Jackson, L.M. Nilsson and P.J. Wyatt, J. Appl. Polym. Sci., 43 (1989) 99.
[24] S.A. Thomson, A.A. Protter, L. Bitting, J.C. Fiddes and J.A. Abraham, Methods Enzymol., 198C (1991) 96–116.
[25] H. Ago, Y. Kitagawa, A. Fujishima, Y. Matsuura and Y. Katsube, J. Biochem., 110 (1991) 360.